

Article

Comparative Estimation of Urban Development in China's Cities Using Socioeconomic and DMSP/OLS Night Light Data

Junfu Fan^{1,2}, Ting Ma^{1,*}, Chenghu Zhou¹, Yuke Zhou¹ and Tao Xu^{1,3}

¹ State Key Laboratory of Resources and Environmental Information System, Institute of Geographical Sciences and Natural Resources Research, Chinese Academy of Sciences, Beijing 100101, China; E-Mails: fanjf@lreis.ac.cn (J.F.); zhouch@lreis.ac.cn (C.Z.); zyk@lreis.ac.cn (Y.Z.); xutao@lreis.ac.cn (T.X.)

² School of Architectural Engineering, Shandong University of Technology, Zibo 255049, China

³ University of Chinese Academy of Sciences, Beijing 100049, China

* Author to whom correspondence should be addressed; E-Mail: mting@lreis.ac.cn; Tel.: +86-10-6488-8960; Fax: +86-10-6488-9630.

Received: 24 June 2014; in revised form: 29 July 2014 / Accepted: 12 August 2014 /

Published: 22 August 2014

Abstract: China has been undergoing a remarkably rapid urbanization process in the last several decades. Urbanization is a complicated phenomenon involving imbalanced transformation processes, such as population migrations, economic advancements and human activity dynamics. It is important to evaluate the imbalances between transformation processes to support policy making in the realms of environmental management and urban planning. The Defense Meteorological Satellite Program's Operational Linescan System (DMSP/OLS) nighttime lights time series imagery provides a consistent and timely measure to estimate socioeconomic dynamics and changes in human activity. In this study, we jointly compared the annual ranks of three variables: the population, the gross domestic product (GDP) and the sum of weighted DMSP/OLS nighttime lights to estimate spatial and temporal imbalances in the urbanization processes of 226 cities in China between 1994 and 2011. We used ternary plots and a Euclidean distance-based method to quantitatively estimate the spatial and temporal imbalances between cities and to classify diverse urban development patterns in China. Our results suggest that, from 1994 to 2011, the imbalances of urbanization processes observed in the eastern, western and middle cities decreased, respectively, by 35.26%, 29.04% and 25.84%; however, imbalances in the northeast increased by 33.29%. The average decrement in imbalances across all urbanization processes in the 226 cities was 17.58%. Cities in the eastern region displayed relatively

strong attractions to population, more rapid economic development processes and lower imbalances between socioeconomic and anthropogenic dynamics than cities in other regions. Several types of urban development patterns can be identified by comparing the morphological characteristics of temporal ternary plots of the 226 cities in China. More than one third (35.40%) of the 226 cities presented balanced states during the period studied; however, the remainder showed alternative urban development patterns.

Keywords: urbanization; imbalance; night light; ternary plot; China

1. Introduction

At present, approximately 0.5% of the Earth's land surface is composed of urban areas [1], accounting for approximately 52.1% of the global population [2]. Urbanization is a complex phenomenon accompanied by rural-urban transitions [3], population migrations [4–6] and transfers of matter and energy [7,8]. Urban areas are hot spots that lead to environmental changes at multiple scales [9], and urbanization poses both challenges and opportunities for sustainable development and environmental management [10]. The velocity or frequency of such dynamics exhibits human activity intensities in urban areas, such as energy consumption, infrastructure construction and socioeconomic activity [11]. In general, cities with similar population and socioeconomic parameter scales (e.g., gross domestic product, or GDP; income) should represent approximately equal intensities of human activity. However, the three indicators could be imbalanced, which would lead to spatial and temporal disparities between cities distributed at a large scale, as they are in China [12]. Most cities in China have been experiencing rapid urbanization in the last two decades [11,13,14]. The balance between population, socioeconomic parameters and human activity may affect policy making for cities' sustainable development. Consequently, it is necessary to evaluate the spatial and temporal balance patterns of China's cities to support policy making in environmental management and urban planning in response to the remarkably rapid, large-scale urbanization processes occurring worldwide [15,16].

Population and GDP, which are always derived from official census and statistical data, are critical indicators used to evaluate the urbanization level of cities. Traditional census data, socioeconomic statistical data and sample survey data were widely used in previous works to assess differences in development between cities. Smith analyzed third world cities in a global perspective using official statistical data and took Nigeria, East Asia and South Korea as examples to explain the relationship between uneven urbanization processes and local policies [17]. Fujita and Hu examined trends in regional disparities in China using GDP and industry output data [18]. Deng *et al.* estimated the extent of cities and the factors driving urban expansion in China from the 1980s to 2000 using high-resolution satellite imagery and socioeconomic data and found that the growth of income was the driving factor in China's urban expansion [13]. In spite of the notable capability of accurately depicting gross demographic and socioeconomic dynamics, census and statistical socioeconomic data are always characterized by relatively high cost, low temporal resolution and the probable inclusion of artificial errors [19]. Furthermore, census and statistical data cannot reflect the detailed spatial characteristics of urbanization processes and anthropogenic activity intensities, such as the increase in impervious

surfaces and the establishment of infrastructure and are, therefore, insufficient for evaluating the spatial and temporal balance of rapidly developing cities.

Remotely sensed nighttime light imagery derived from the Defense Meteorological Satellite Program's Operational Linescan System (DMSP/OLS) provides a straightforward way to analyze the relationship between urbanization and anthropogenic activities [11] and has been extensively used in urban studies. Due to the unique capability of DMSP/OLS to detect low levels of visible and near-infrared nighttime radiance signals, the composed stable nighttime light data have been used for mapping urban areas [20–23], estimating the spatial sprawl trends of cities [24] and measuring socioeconomic activity and dynamics [19,25]. In addition, nighttime light imagery can be a primary data source to evaluate GDP growth [11], energy consumption [26], population density and agglomeration [27], energy density [28] and human wellbeing [29] at multiple levels to estimate the role that anthropogenic activity plays in urbanization processes. Although there is no single valid brightness threshold used to differentiate urban and non-urban areas, due to the inconsistent relationship between the actual lighted area and urban boundaries resulting from over-glow or “blooming” effects [21], previous studies commonly suggest that DMSP/OLS night radiance data could be indicative of urbanization-related socioeconomic activity, especially in the absence of census data [11,19]. Highly urbanized areas are associated with larger populations and more intense socioeconomic activity than less-developed regions. It can be inferred that cities with similar populations and economic parameters should represent homologous intensities of human activity, which could be observed using the nighttime light data. Given its easy access, low cost and integrity of spatial cover, the long-term DMSP/OLS night light data, therefore, offer great potential as a supplement to census and statistical socioeconomic datasets for estimating spatial and temporal equality of cities at multiple scales.

Although great emphasis has been placed on estimating differences in urbanization, previous studies have rarely attempted to examine the spatial and temporal imbalances of urbanization processes using the combination of demographic, socioeconomic and anthropogenic indicators. The objectives of this paper are to estimate the spatial and temporal imbalances of urbanization processes in China's cities at regional and city levels using a distance method based on ternary plot and the combined comparisons of annual ranks of three variables: population, GDP and the sum of weighted DMSP/OLS nighttime lights. We conducted a series of pixel statistics, normalization and ternary plot-based Euclidean distance calculations for 226 China's cities to evaluate spatial and temporal balance from the local to the regional level and attempted to investigate and summarize the different categories of urban growth patterns of cities in China during the period of 1994–2011.

2. Data and Methods

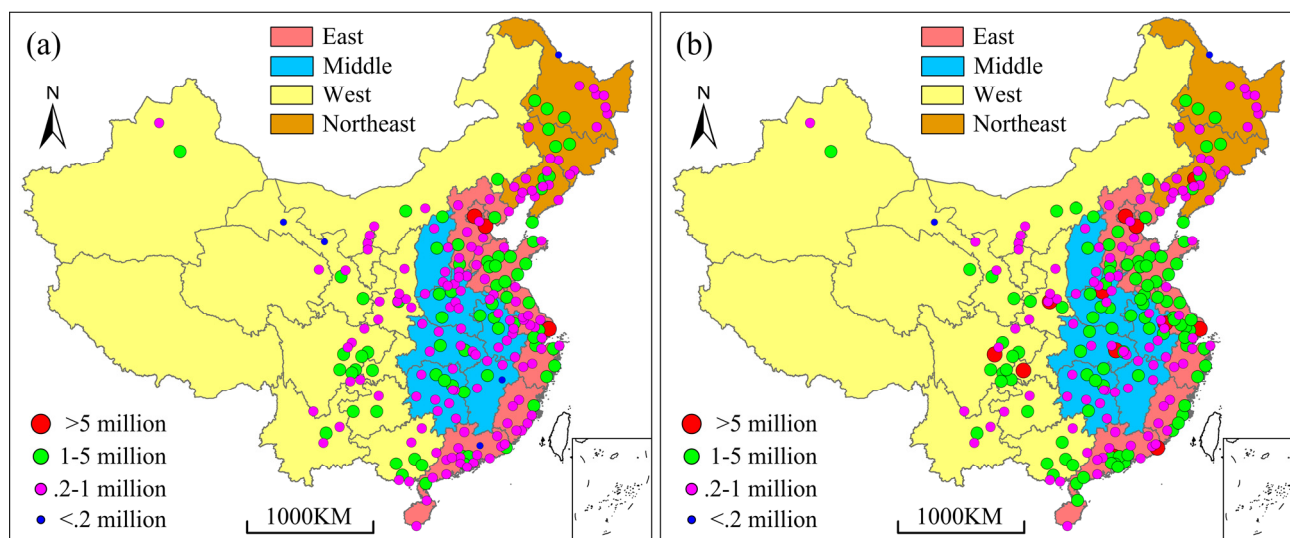
China has been experiencing unprecedented urbanization over the last several decades [13,30]. The rapid economic growth of China is not only associated with the large-scale migration of people into cities [6], but is also connected with many environmental and social consequences, such as urban heat islands (UHI) [30], increased health exposure risks [31] and enhanced regional disparities of cities [12]. Investigating the spatial and temporal imbalances between cities is crucial for the sustainable development of China in the context of policy making. The combination of socioeconomic

data and DMSP/OLS nighttime light data provided a substantive approach to estimating the spatial and temporal differentiations between China's cities.

2.1. Demographic and Socioeconomic Data

We assembled a time series of statistical data on urban population and GDP spanning 18 years (1994–2011) for 226 of China's prefectural-level cities and municipalities derived from official statistical yearbooks [32] and the national sixth census datasets [33]. The 226 cities are distributed in most province-level cantons with the exception of 4 for the lack of statistical data: Tibet, Taiwan, Marco and Hong Kong. To estimate regional differences in urbanization processes in China, the 226 cities are divided into 4 regional groups according to the National Bureau of Statistics of China, the east, the middle, the west and the northeast, as shown in Figure 1. The demographic and economic data were collected from statistical areas defined as urban by the National Bureau of Statistics of China and excluded suburban areas. The time series of the sum of weighted nighttime lights for China's cities are collected in the same statistical urban areas.

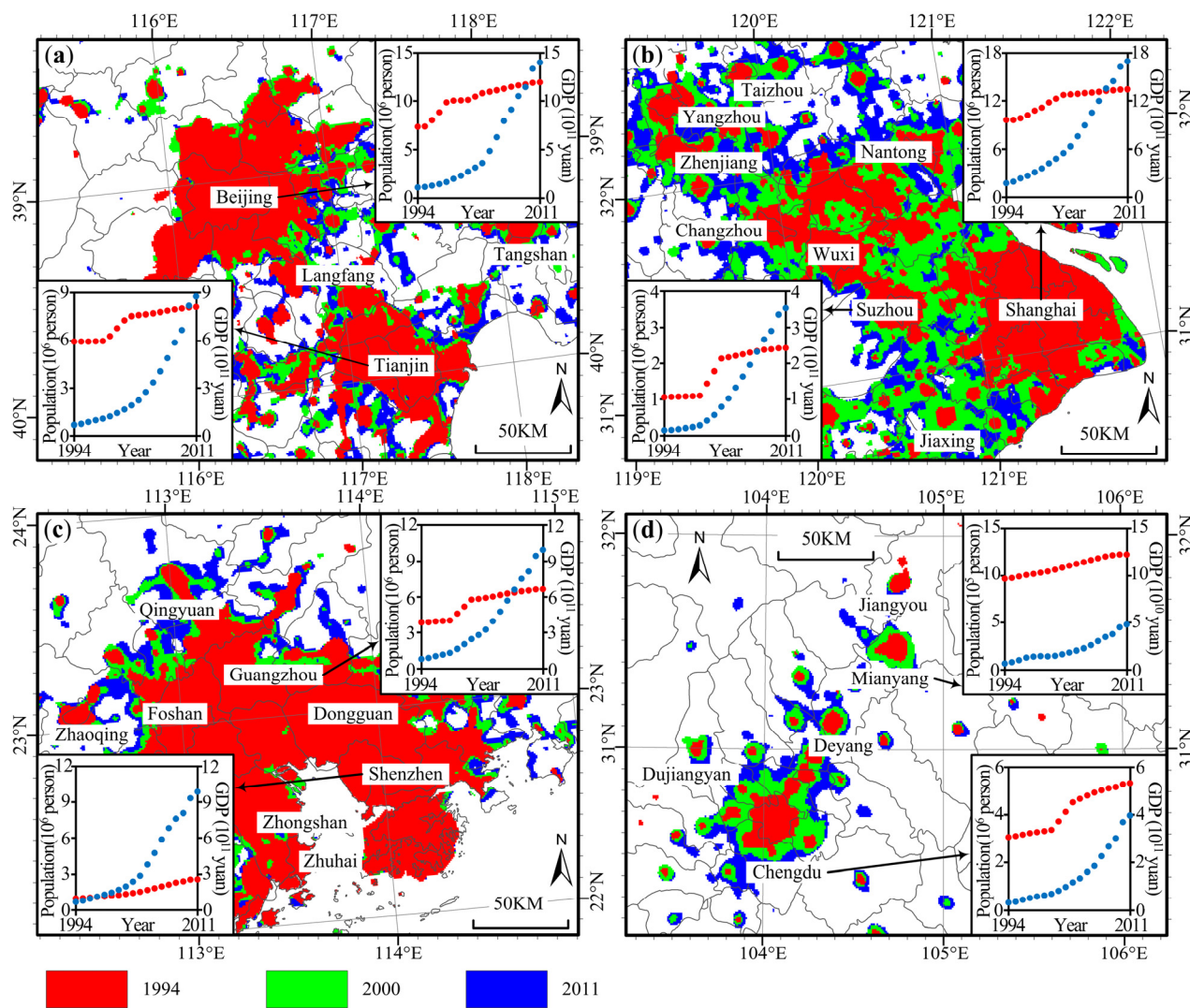
Figure 1. Spatial distribution of China's prefectural-level cities and municipalities grouped by the population sizes in 1994 (a) and 2011 (b).



2.2. DMSP/OLS Nighttime Light Imageries

The version 4 composed stable nighttime light (NTL) data, derived from the visual band of the DMSP/OLS sensors onboard polar orbiting platforms, are ideal for annual and continuous estimation of changes in the intensity of anthropogenic activity [11] and differentiation of urbanization processes [34], as shown in Figure 2. The nighttime light images were archived and provided digitally from 1992 to 2012 by the National Oceanic and Atmospheric Administration's National Geophysical Data Center (NOAA/NGDC). These images are grid-based annual data compositions with a 0–63 digital number (DN) and a 30 arc-second (approximately 1 km at the equator) spatial resolution for pixels.

Figure 2. Spatio-temporal dynamics in the Defense Meteorological Satellite Program’s Operational Linescan System (DMSP/OLS) night light area and statistical data trends for China’s cities located in 4 major metropolitan areas between 1994 (red), 2000 (green) and 2011 (blue): (a) Beijing-Tianjin area; (b) Yangtze River Delta; (c) Perl River Delta; (d) Sichuan province. Solid curves are administrative boundaries.



In this study, the nighttime light time series datasets were collected by 6 individual sensors: F10 (1994), F12 (1995–1997, 1999), F14 (1998 and 2003), F15 (2000–2002, 2004 and 2006), F16 (2005, 2007–2009) and F18 (2010 and 2011). The second-order regression model and a series of parameters provided by Elvidge *et al.* are used annually to empirically intercalibrate the NTL images, which are matched with the composite of F12 in 1999 to minimize the effects of variation among sensors [35].

The DMSP/OLS NTL data can lead to the overestimation of urbanization [20,34], and there is no single valid brightness threshold for extracting the lit area of cities distributed across a large scale. Despite the limitations associated with applying nighttime light imagery (e.g., over-glow or shrink effects) [11,21] when quantitatively assessing the actual extent of urban areas, DMSP/OLS nighttime lights data provide a consistent and timely measure to characterize different categories of urbanization processes. In this study, we used the sum of weighted night lights as one of the 3 combined indicators

to estimate the degree of imbalance in a city. The sum of weighted night lights is defined as the sum of DN values multiplied by the ratio of trapezoid area of a pixel to the average area of all pixels that are located in its administrative districts (excluding suburban areas) and which also can be illustrated by Equation (1); furthermore, pixels with $DN < 12$ were excluded when calculating the sum of weighted night lights, in accordance with Ma *et al.*, to reduce the overestimation effects caused by low lights [11]. In Equation (1), DN_{pixel} and $Area_{pixel}$ are the DN value and trapezoid area of each pixel, $Area_{sum}$ is the sum of trapezoid area values of all calculated pixels and n is the pixel number.

$$Weighted\ NTL_{sum} = \frac{\sum (DN_{pixel} \times Area_{pixel})}{Area_{sum} / n} \quad (1)$$

2.3. Ternary Plots and the Euclidean Distance-Based Classification Method

The time series of ranks of population, GDP and the sum of weighted night lights of the 226 cities in question from 1994 to 2011 were calculated and normalized according to Equation (2).

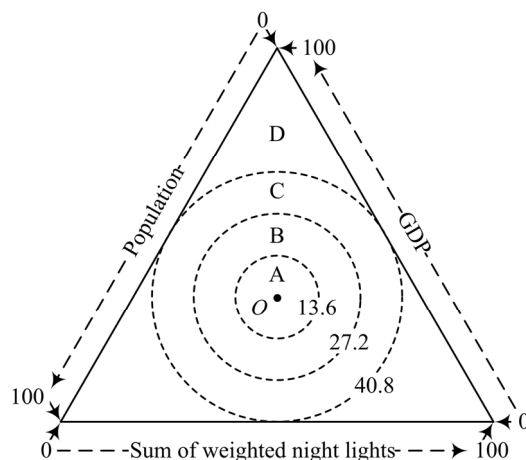
$$\begin{cases} V_{POP} = \frac{R_{POP}}{R_{POP} + R_{GDP} + R_{NTL}} \times 100\% \\ V_{GDP} = \frac{R_{GDP}}{R_{POP} + R_{GDP} + R_{NTL}} \times 100\% \\ V_{NTL} = \frac{R_{NTL}}{R_{POP} + R_{GDP} + R_{NTL}} \times 100\% \end{cases} \quad (2)$$

In Equation (2), R_{POP} , R_{GDP} and R_{NTL} represent population ranks, GDP ranks and the sum of weighted night lights ranks, respectively, of the 226 cities in a particular year; V_{POP} , V_{GDP} and V_{NTL} represent the normalized values of the three variables, the combinations of which were used as coordinate values to plot the ternary diagrams, as shown in Figure 3. Each point on the ternary diagram represents an urbanization status for a city in a particular year. Theoretically, if a city was in a balanced urbanization process in a certain period, the ranks of its three parameters should be close or approximately equal; therefore, the point drawn on the ternary plot should be very close to the center point O . Conversely, points away from O on the triangle graph represent cities with an imbalanced development status. As shown in Figure 3, the three equally spaced concentric circles divide the ternary plot into four sections, which represent four urbanization statuses according to distance from point O : A represents the most balanced, B is less balanced, C represents the imbalanced urbanization status and D is the most imbalanced. The ternary distance between a city point on the ternary plot and point O can be calculated according to Equation (3).

$$\begin{cases} d = \sqrt{(V_{POP} - V_{POP}^O)^2 + (V_{GDP} - V_{GDP}^O)^2 + (V_{NTL} - V_{NTL}^O)^2} \\ V_{POP}^O = V_{GDP}^O = V_{NTL}^O = 100 / 3 \end{cases} \quad (3)$$

The ternary plot revealed that the main factor leading to the imbalances is when points fall into parts C and D. Therefore, the ternary plot and ternary distance provided a potential approach to investigating the imbalances, differences and disparities between cities in a certain year or to compare different urbanization processes within a city over a long period of time.

Figure 3. Ternary plot and four types of urbanization processes divided by three equal spacing concentric circles defined by Euclidean distance to point O (the center of the triangle).



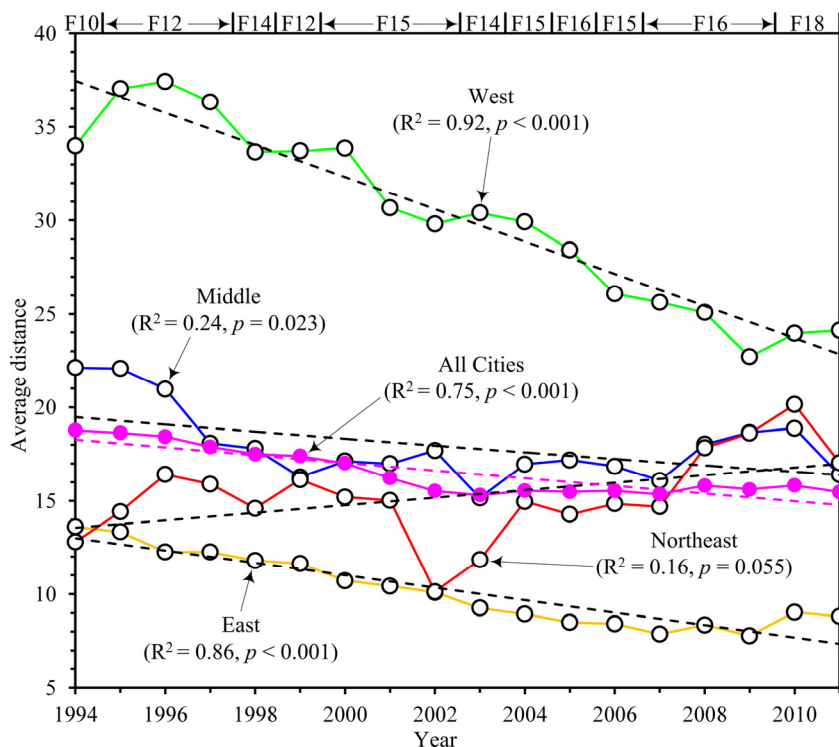
3. Results and Discussion

3.1. Estimation of Urbanization Imbalances and Disparities

City development is accompanied by many social phenomena, such as population dynamism, economic growth and the construction of infrastructure, all of which complicate the estimation of urbanization processes. It is well documented that China has been experiencing rapid urbanization since the 1990s with extensive rural-urban migrations and vigorous economic growth. Public policies, location and natural resources are potential factors leading to differentiation in the urbanization processes of China's cities, especially in different regions (as shown in Figure 2). Differences between cities can be represented as disparities or imbalances of socioeconomic and nighttime light variables. For example, cities playing the role of economic center may attract many people and exhibit correspondingly higher ranks in terms of GDP sum of nighttime lights. However, cities that produce certain natural resources, such as coal, oil or gas, may have high economic ranks but low ranks in terms of population and nighttime lights. The disparities between the three parameters of a city—population, GDP and the sum of nighttime lights—indicate an imbalanced urbanization process, which can be represented on the ternary diagrams using the distance factor.

In this study, the 226 cities were divided into four regional groups: the east (including Beijing, Tianjin, Shanghai and cities in Hebei, Shandong, Jiangsu, Zhejiang, Fujian, Guangdong and Hainan provinces), the middle (including cities in Shanxi, Henan, Anhui, Hubei, Hunan and Jiangxi provinces), the west (including Chongqing and cities in Xinjiang, Qinghai, Gansu, Inner Mongolia, Ningxia, Shaanxi, Sichuan, Yunnan, Guangxi and Guizhou provinces) and the northeast (including Heilongjiang, Jilin and Liaoning provinces). We calculated the annual average regional Euclidean distances of cities in the four regions from 1994 to 2011 using the ternary plot method, as illustrated by Equation (3) and Figure 3. To investigate the variation trends of the average distances, we estimated regression parameters of a linear model using the least squares method. In this method, the “x” parameter is year and the “y” parameter is the average distance values of each year. The analyses and variation trend fitting results are illustrated in Figure 4.

Figure 4. Annual variations of regional average ternary distance changes of China's cities from 1994 to 2011.

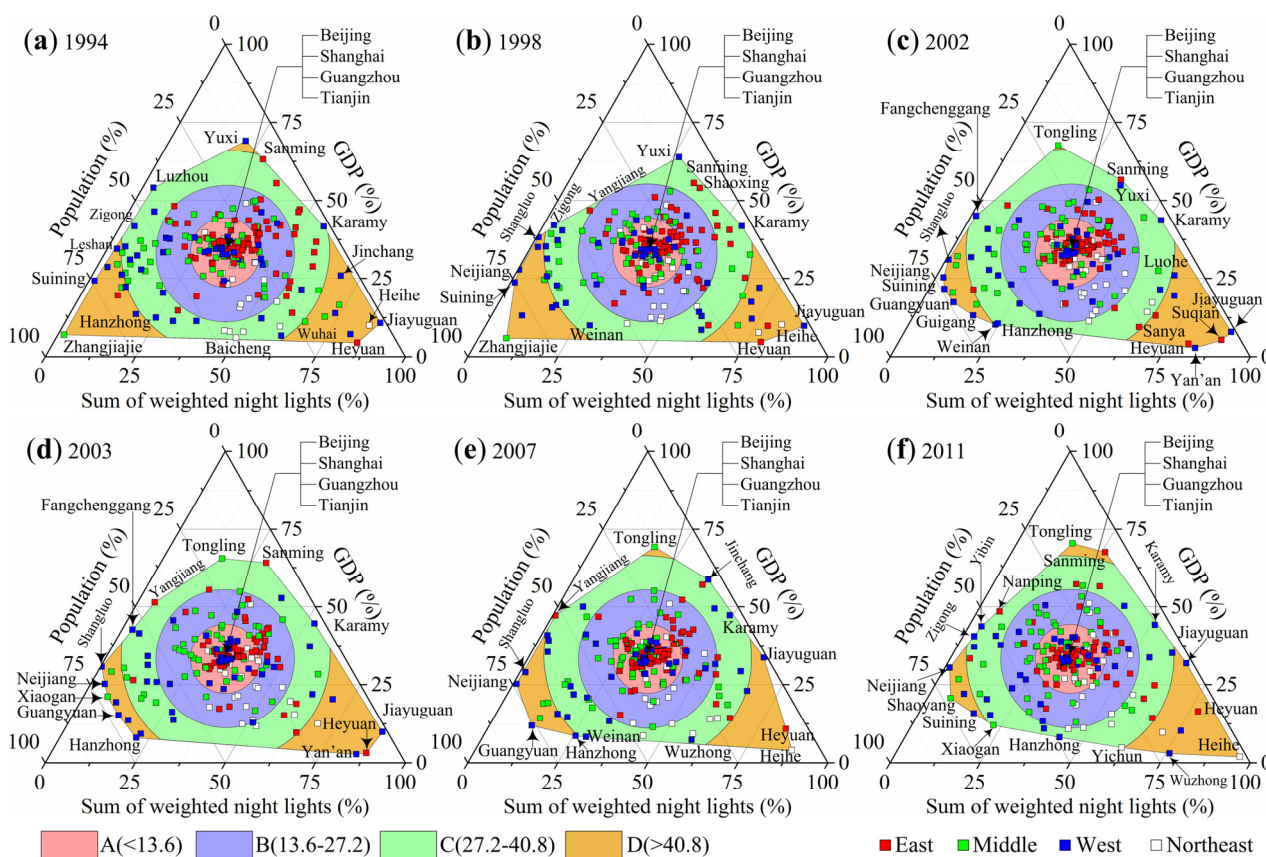


As shown in Figure 4, R^2 is the coefficient of determination, which is a measure of goodness-of-fit; the significance of regression was tested using t -statistics with the null hypothesis. Our results indicated that the general average imbalance trend of all samples (cities) gradually declined, but there were distinct differences between the four regions in the period of 1994–2011. The average ternary distance of the cities in the east region of China maintained the lowest level of values and decreased from 13.60 to 8.81 simultaneously with $R^2 = 0.86$ ($p < 0.001$). The average distance of the cities on the ternary plot in the west region diminished from 33.99 to 24.12 with the highest coefficient of determination being 0.92 ($p < 0.001$); however, the distance values in this region remained relatively high in each year from 1994 to 2011. Our results also revealed that the variations in average distances in the middle and northeast regions were complicated and that both displayed small coefficients of determination (less than 0.25). The distances in the middle region remained nearly constant (especially from 1997 to 2011) and increased in the northeast region from 12.79 to 17.04. The complicated variation characteristics of northeastern cities were closely related with their historical position and functional specializations in China's economic development process. However, it was difficult to quantitatively estimate the accurate spatio-temporal characteristics in this region, which needed more detailed socioeconomic data and more sample cities. It could be deduced from our results that there were evident differentiations between cities in this region, especially cities with different population sizes and economy scales.

These results may indicate that the urbanization processes of cities in the east and west regions of China trended toward more balance. Imbalances and disparities between socioeconomic parameters and human activity of cities in the two regions declined continuously, albeit at different rates, and the west demonstrated higher velocities, but lower changing ratios. The imbalance decrement of eastern

cities was 35.26%, while that of western cities was 29.04%. Therefore, during the period of 1994–2011, cities in the east region were relatively more mature and urbanizing at a relatively faster rate; the corresponding characteristics of the urbanization processes of western cities were rapid, intense and at a relatively low level. The balance of cities in the middle region increased by 25.85%, indicating that cities in this region were undergoing urbanization processes with the slowest dynamics; in the northeast region, imbalances and disparities in the urbanization processes of cities increased by approximately 33.29%. The average decrement of the overall imbalances within the urbanization processes of the 226 cities was 17.58% from 1994 to 2011. However, specific characteristics of disparities in certain cities cannot be ascertained from the above results. To estimate the specific imbalance characteristics, we plotted all of the cities on ternary diagrams for a period of six years, as shown in Figure 5.

Figure 5. Ternary plots and classification statuses of 226 China’s cities in 1994 (a), 1998 (b), 2002 (c), 2003 (d), 2007 (e) and 2011 (f) based on the Euclidean distance method.



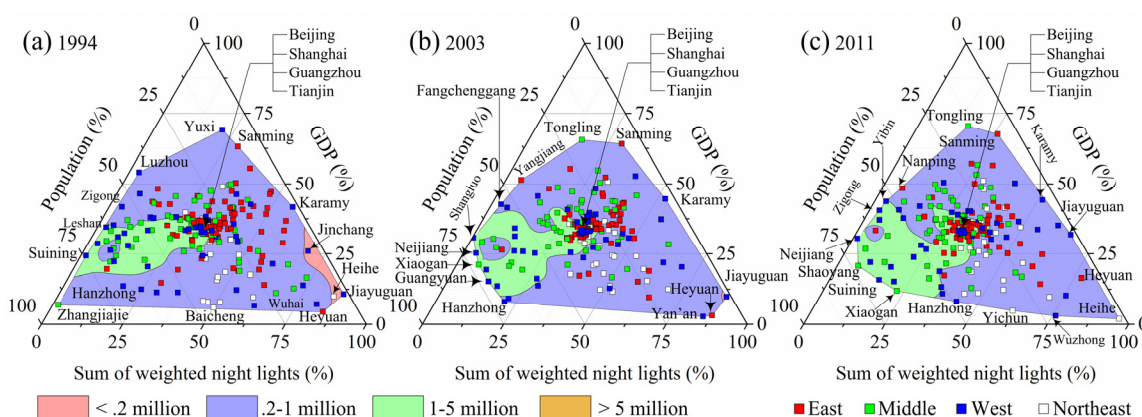
The results demonstrated that the convex hull of all city points on the ternary plots shrank to some extent from 1994 to 2011, indicating that the general imbalances of all cities decreased. Particularly, shrinking on the left-bottom of the convex polygon implied that imbalances caused by the population and GDP indicators were reduced and the sum of weighted night lights became the main factor, which led to disparities for cities located in this area on the ternary plots, such as Suining, Guangyuan and Zhangjiajie. Most cities in the east region and all of the provincial capitals are concentrated in Area A ($d < 13.6$) on the ternary plots; therefore, imbalances or disparities in the urbanization processes of large cities were evidently lower than those in small cities during the last two decades. Most cities in

the west region are distributed in Areas C and D ($d > 13.6$). Cities in the middle and northeast regions are distributed in the four areas on the triangle graphs. Cities on the boundaries of the convex hull of points on the ternary plots represented differences in urbanization processes in China. Cities on the left, such as Zigong, Neijiang and Shangluo, were developing with moderate population and GDP ranks, but extremely low nighttime lights ranks from 1994 to 2011. It is revealed that the infrastructure development of those cities lagged behind population expansions and economic advancements from 1994 to 2011. In contrast, cities such as Heyuan and Heihe showed that anthropogenic activity dynamics could prevail over socioeconomic changes. Cities on the right, such as Karamy and Jiayuguan, are those that developed with higher ranks in GDP and night lights, but smaller populations, which means that the per capita income or living standard of those cities was at a relatively higher level in China during 1994 to 2011. Thus, our results indicated that there were imbalances among urbanization processes and disparities between socioeconomic dynamics and human activities. The ternary plots and Euclidean distance-based classification method provided potential approaches to estimate those imbalances and disparities and also to identify different urbanization patterns in China’s cities during the last two decades.

3.2. Socioeconomic Variations and Distribution Characters on Ternary Plots

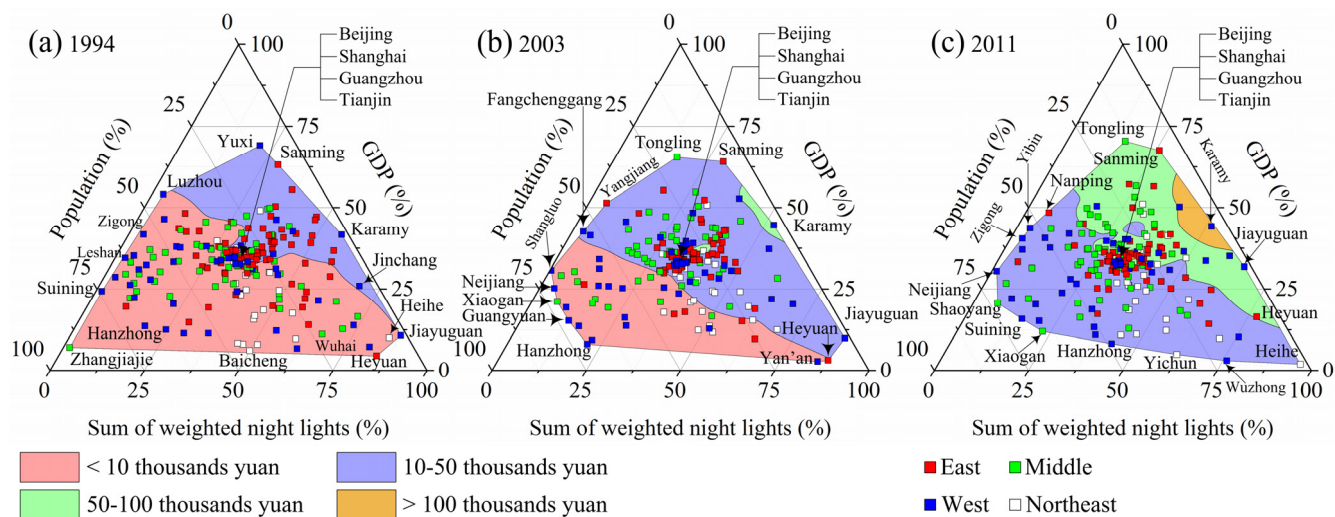
Socioeconomic parameters, such as population and GDP, are the most frequently used indicators to estimate urbanization. As shown in Figure 6, our results indicate that the number of cities with small populations (<0.2 million) declined from 1994 to 2011. With rapid development, regions defined by population contours of 1–5 million also expanded to some extent. Most provincial-level cities, such as Beijing, Shanghai and Guangzhou, are concentrated around the center of the triangle. Cities where population played a dominant role in the ternary indicator system are located in the left-bottom area of the triangles. Such cities usually maintain relatively lower income and infrastructure construction levels. Additionally, cities with relatively high ratios of population or night lights, such as Zhangjiajie in 1994 and Heihe in 2011, could experience extreme distributions on ternary plots; however, GDP would not lead to similar distributions. Therefore, our results revealed that it is difficult for a developing city in China to maintain a relatively small population and low level of total weighted nighttime lights alongside a relatively high level of economic advancements.

Figure 6. Ternary plots with contours of population sizes of China’s cities in 1994 (a), 2003 (b) and 2011 (c).



To investigate the variation trends and imbalances of economic advancements between China’s cities, we chose the indicator of GDP per capita and plotted corresponding ternary contour diagrams in 1994, 2003 and 2011, as shown in Figure 7.

Figure 7. Ternary plots with contours of GDP per capita of China’s cities in 1994 (a), 2003 (b) and 2011 (c).



Similarly, as discussed in relation to the population ternary contour plots, the GDP per capita ternary diagrams also show cascade variation trends. The results shown in Figure 7 demonstrate that the GDP per capita of most of China’s cities was less than 10 thousand CNY in 1994 and rose to 50–100 thousand CNY in 2011, indicating rapid economic advancements associated with China’s urbanization processes. Furthermore, cities in the east region represented relatively strong attractions to population, more rapid economic development processes and fewer imbalances or disparities between the combined ternary indicators. Cities in the west and middle regions demonstrated relatively low levels of economic development and more imbalances or disparities between the three indicators of population, GDP and the sum of weighted night lights. Population and economic variations and imbalances of cities in the northeast of China did not display such evident extremes on the ternary contour plots, as shown in Figures 6 and 7.

3.3. Pattern Classification of Urbanization Processes in China

The rapid urbanization processes in China’s cities were accompanied by variation in socioeconomic dynamics and anthropogenic activities. Variation trends associated with the differing combinations of the three variables of interest—population, GDP and the sum of weighted night lights—led to spatial and temporal disparities and imbalances between cities. The imbalances and disparities between socioeconomic and DMSP/OLS nighttime lights variables differentiate the urbanization processes and are potential indicators for the investigation and classification of urbanization patterns in China’s cities. We took the temporal variation trends of imbalance status, derived from the combination of the three indicators, as the basis of classification of urbanization process patterns. The temporal variation trends could be depicted by the trajectories of cities plotted on the ternary diagrams, from 1994 to 2011.

As shown in Figures 8 and 9, the morphological characteristics of the temporal moving trajectories of 226 cities on the ternary diagrams were used for the classification of urbanization processes in China, and 11 categories of urbanization patterns were found. These 11 categories represent differences in development patterns among China's cities. In concrete terms, approximately 3.98% of China's cities (nine of 226) exhibited a pattern of urbanization characterized by a straight, bottom-to-top trajectory, such as Liaoyuan (Figure 8a), indicating relatively rapid economic advancements, moderate human activity and an extremely low level of population expansion. Only 1.33% of the cities show the Type b pattern with a top-to-bottom trajectory, such as Datong (Figure 8b), and demonstrate reverse urbanization processes. Type c, observed in cities such as Qingyuan and Wuzhong (Figure 8c-1 and 8c-2, respectively), was exhibited by 20.35% of the 226 cities and displayed complex urbanization processes, characterized by alternating increases and decreases in more than one variable.

Type d and Type e patterns demonstrated horizontal left-to-right or right-to-left linear trajectories, as shown in Figure 8d/e (2.65%/5.75%), indicating that cities such as Zhoushan and Maoming were urbanized with relatively rapid population dynamics and strong intensity of human activities (e.g., infrastructure constructions), but steady economic advancements during 1994–2011. Approximately 8.85% of China's cities, such as Leshan (Type f, Figure 8f), exhibited conspicuously repeated and complicated temporal trajectories on the ternary plots, indicating possible diapause during the course of urbanization. Approximately 35.40% of the samples maintained extraordinary balance states among the three variables in the past two decades, as evidenced by the concentration of annual points around with the center on the triangle plots (Type g, Figure 8g). The Type h pattern was displayed by 1.33% of the cities and is characterized by a left-bottom to right-top linear trajectory, which means that cities, such as Longyan (Figure 8h), experienced relatively rapid changes in nighttime lights, but lower rates of population change. Similarly, cities exhibited linear patterns characterized by a right-top to left-bottom trajectory (Type i, like Zhuhai in Figure 8i, 10.18% of sample), left-top to right-bottom (Type j, like Suining in Figure 8j, 7.52% of sample) and right-bottom to left-top (Type k, like Baoding in Figure 8k, 2.65% of sample), indicating a series of homologous variation trends on the parameter combinations of population, GDP and the sum of weighted nighttime lights.

There are spatial differences among the four regions within the urbanization process classifications. As shown in Figure 9, most of the cities in the east region demonstrated Type g (34 cities or 40.96%) and Type i (16 cities or 19.28%) patterns, indicating that cities in the east region maintained or achieved balanced states among the three parameters in 2011. Most cities in the middle region conformed to Type g (19 cities or 32.2%) and Type c (13 cities or 22.03%) urbanization patterns during 1994–2011. Types c (15 cities or 29.41%) and g (13 cities or 25.49%) were the primary patterns in the west region, as well. In the northeast region, cities exhibiting Type g (14 cities or 42.42%) and The Type c (seven cities or 21.21%) urbanization pattern were also in the majority.

Figure 8. Eleven categories of different urbanization patterns: bottom to top (a), top to bottom (b), circle or half circle (c-1, c-2), left to right (d), right to left (e), reciprocate (f), central (g), left-bottom to right top (h), right-top to left-bottom (i), left-top to right-bottom (j) and right-bottom to right-top (k) of China’s cities.

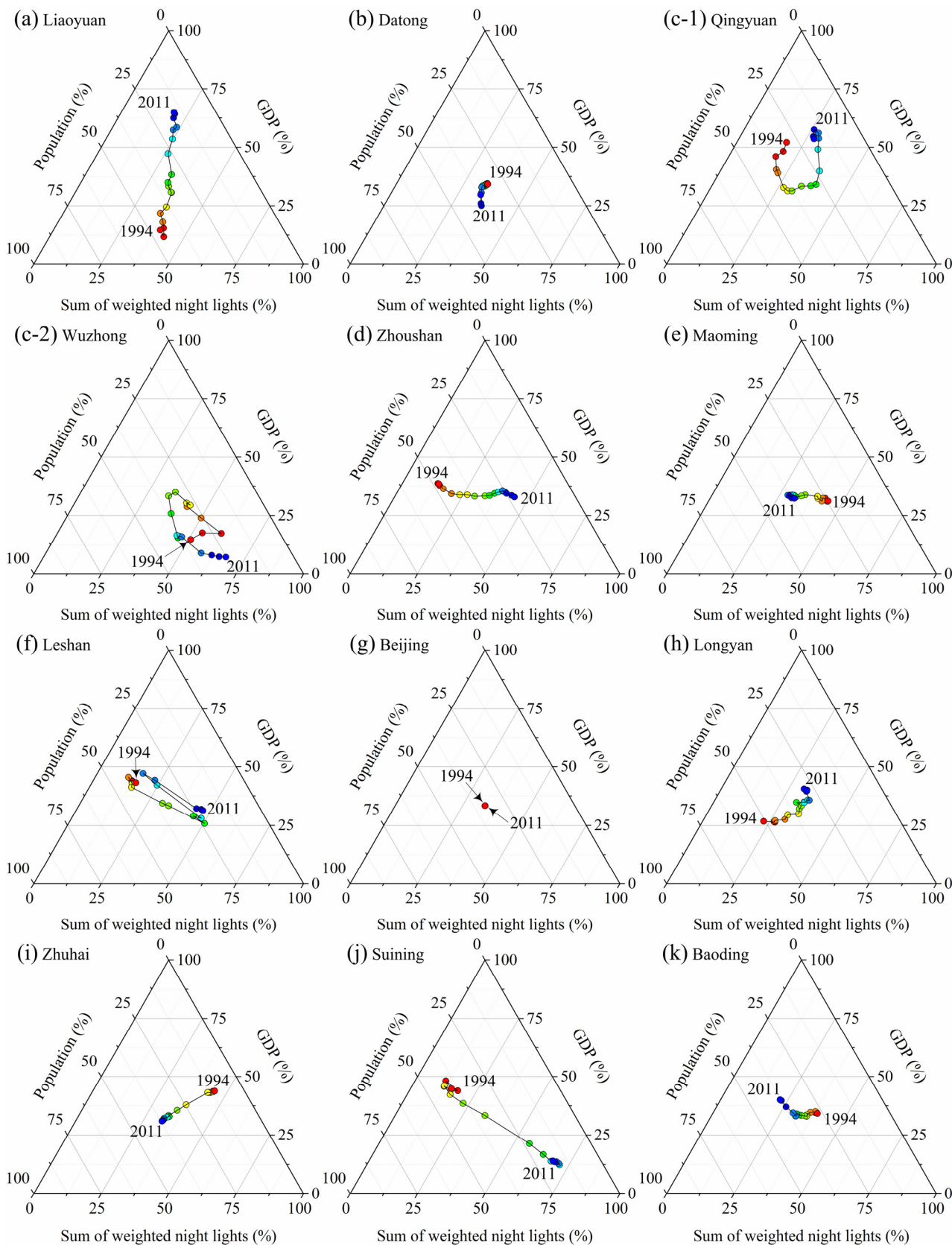
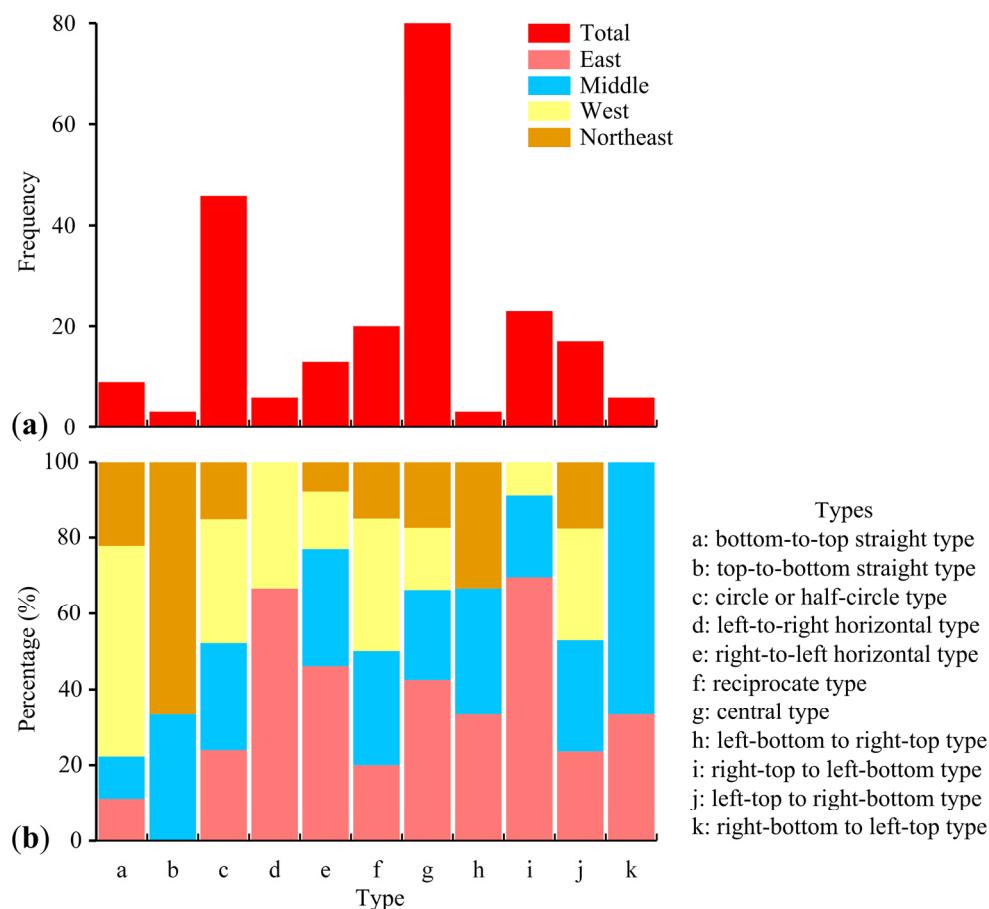


Figure 9. (a) Total frequency of urbanization process patterns of China’s cities. (b) Distribution of urbanization process patterns in east, middle, west and northeast China.



4. Conclusions

China has been undergoing a rapid urbanization accompanied by different patterns of transformation processes in the last several decades. However, no single urbanization process can account for the complicated socioeconomic and anthropogenic dynamics that occurred in different regions at a large scale [34].

In this paper, we systematically estimated the spatial and temporal imbalances between urbanization processes of China’s cities at regional and city levels using a series of ternary plots based on a comparison of annual ranks of three variables: population, GDP and the sum of weighted DMSP/OLS nighttime lights. Furthermore, morphological character dynamics of temporal imbalances demonstrated on ternary diagrams were investigated as the bases for the classification of different urbanization process patterns. According to our results, there were spatial and temporal imbalances between the urbanization processes of China’s cities in the period of 1994–2011.

First, the urbanization processes of cities in the east and west regions of China trended toward more balanced phases, while cities in the middle and the northeast regions exhibited complicated variation trends. From 1994 to 2011, imbalances and disparities between socioeconomic parameters and human activity of cities changed continuously and at different speeds in China: the imbalances of eastern, western and middle cities decreased, respectively, by 35.26%, 29.04% and 25.84%; however,

imbalances in northeastern cities increased by 33.29%. The average decrement of the overall imbalances within urbanization processes of the 226 Chinese cities was 17.58%.

Second, the ternary contour plots of socioeconomic variables, such as the population and the GDP per capita, showed cascade variation trends. The results revealed that the imbalances or disparities in the urbanization processes of China's cities increased with cascade characteristics from the east region to the west region. Furthermore, cities in the east region exhibited a relatively strong attraction to population, more rapid economic development processes and fewer imbalances. Cities in the middle and, especially, west regions demonstrated relatively low levels of economic development and greater imbalances between the three combined indicators. Such characteristics were not evident in the urbanization processes of cities in northeastern China.

Third, the urbanization processes of the 226 Chinese cities could be classified into 11 categories by comparing the morphological characteristics of temporal ternary graphs of single cities. More than one third of the cities displayed balanced states (Type g, 35.40%) in their urbanization processes from 1994 to 2011. The rest of the cities demonstrated 10 different types of urbanization patterns. There were spatial differences between the four regions with regard to the urbanization process classifications. Most of the cities in the east (34 cities or 40.96%), middle (19 cities or 32.2%) and northeast (14 cities or 42.42%) regions showed a Type g pattern. Type c (15 cities or 29.41%) was the primary pattern in the west region.

Using a combination of socioeconomic variables and DMSP/OLS nighttime light data can improve the ability to identify the imbalance or disparity trajectories of urbanization processes. However, challenges remain, most notably in the elimination of over-glow and shrink effects for accurate extraction of urbanized areas from DMSP/OLS images and in fine-tuning the quantitative analysis of imbalances or disparities between complicated urbanization processes. Further studies are needed to expand the application of DMSP/OLS nighttime light data to estimate urban growth patterns at multiple scales over a longer period.

Acknowledgments

This research has been funded by the National Natural Science Foundation of China (No. 41371379 and No. 41171307), Key Programs of the Chinese Academy of Sciences (No. KZZD-EW-07) and National Key Technology R&D Program (No. 2011BAH24B10). We would like to gratefully thank the anonymous reviewers for their insightful and helpful comments to improve the manuscript.

Author Contributions

Junfu Fan collected and processed the data, performed analysis and wrote the paper. Ting Ma and Chenghu Zhou conceived and designed the study and methods. Yuke Zhou and Tao Xu contributed to analysis and interpretation of the data.

Conflicts of Interest

The authors declare no conflict of interest.

References

1. Schneider, A.; Friedl, M.A.; Potere, D. A new map of global urban extent from MODIS satellite data. *Environ. Res. Lett.* **2009**, *4*, 044003.
2. World Urbanization Prospects: The 2011 Revision. Available online: <http://esa.un.org/unup/Documentation/faq.htm> (accessed on 20 August 2014).
3. Xu, C.; Liu, M.; Zhang, C.; An, S.; Yu, W.; Chen, J.M. The spatiotemporal dynamics of rapid urban growth in the Nanjing metropolitan region of China. *Landsc. Ecol.* **2007**, *22*, 925–937.
4. Ledent, J. Rural-urban migration, urbanization, and economic development. *Econ. Dev. Cult. Chang.* **1982**, *30*, 507–538.
5. Henderson, V. The urbanization process and economic growth: The so-what question. *J. Econ. Growth* **2003**, *8*, 47–71.
6. Zhang, K.H.; Song, S. Rural-urban migration and urbanization in China: Evidence from time-series and cross-section analyses. *China Econ. Rev.* **2003**, *14*, 386–400.
7. Jones, D.W. How urbanization affects energy-use in developing countries. *Energy Policy* **1991**, *19*, 621–630.
8. Francis, T.B.; Schindler, D.E.; Fox, J.M.; Seminet-Reneau, E. Effects of urbanization on the dynamics of organic sediments in temperate lakes. *Ecosystems* **2007**, *10*, 1057–1068.
9. Grimm, N.B.; Faeth, S.H.; Golubiewski, N.E.; Redman, C.L.; Wu, J.; Bai, X.; Briggs, J.M. Global change and the ecology of cities. *Science* **2008**, *319*, 756–760.
10. SEDAC. Global Rural-Urban Mapping Project (GRUMP), v1. Available online: <http://www.sedac.ciesin.columbia.edu/data/collection/grump-v1> (accessed on 14 April 2014).
11. Ma, T.; Zhou, C.; Pei, T.; Haynie, S.; Fana, J. Quantitative estimation of urbanization dynamics using time series of DMSP/OLS nighttime light data: A comparative case study from China's cities. *Remote Sens. Environ.* **2012**, *124*, 99–107.
12. Pedroni, P.; Yao, J. Regional income divergence in China. *J. Asian Econ.* **2006**, *17*, 294–315.
13. Deng, X.; Huang, J.; Rozelle, S.; Uchida, E. Growth, population and industrialization and urban land expansion of China. *J. Urban Econ.* **2008**, *63*, 96–115.
14. Lichtenberg, E.; Ding, C. Local officials as land developers: Urban spatial expansion in China. *J. Urban Econ.* **2009**, *66*, 57–64.
15. Chen J. Rapid urbanization in China: A real challenge to soil protection and food security. *CATENA* **2007**, *69*, 1–15.
16. Liu, Y.; He, S.; Wu, F.; Webster, C. Urban villages under China's rapid urbanization: Unregulated assets and transitional neighbourhoods. *Habitat Int.* **2010**, *34*, 135–144.
17. Smith, D.A. *Third World Cities in Global Perspective: The Political Economy of Uneven Urbanization*; Westview Press: Cumnor Hill, Oxford, UK, 1996.
18. Fujita, M.; Hu, D. Regional disparity in China 1985–1994: The effects of globalization and economic liberalization. *Ann. Reg. Sci.* **2001**, *35*, 3–37.
19. Ghosh, T.; Powell, R.L.; Elvidge, C.D.; Baugh, K.E.; Sutton, P.C.; Anderson, S. Shedding light on the global distribution of economic activity. *Open Geogr. J.* **2010**, *3*, 148–161.

20. Elvidge, C.D.; Baugh, K.E.; Kihn, E.A.; Kroehl, H.W.; Davis, E.B. Mapping city lights with nighttime data from the DMSP operational linescan system. *Photogramm. Eng. Remote Sens.* **1997**, *63*, 727–734.
21. Small, C.; Pozzi, F.; Elvidge, C.D. Spatial analysis of global urban extent from DMSP-OLS night lights. *Remote Sens. Environ.* **2005**, *96*, 277–291.
22. Zhang, Q.; Seto, K.C. Mapping urbanization dynamics at regional and global scales using multi-temporal DMSP/OLS nighttime light data. *Remote Sens. Environ.* **2011**, *115*, 2320–2329.
23. Zhou, Y.; Smith, S.J.; Elvidge C.D.; Zhao, K.; Thornson, A.; Imhoff, M. A cluster-based method to map urban area from DMSP/OLS nightlights. *Remote Sens. Environ.* **2014**, *147*, 173–185.
24. Sutton, P.C. A scale-adjusted measure of “urban sprawl” using nighttime satellite imagery. *Remote Sens. Environ.* **2003**, *86*, 353–369.
25. Doll, C.N.H.; Muller, J.-P.; Morley, J.G. Mapping regional economic activity from night-time light satellite imagery. *Ecol. Econ.* **2006**, *57*, 75–92.
26. Amaral, S.; Câmara, G.; Monteiro A.M.V.; Quintanilha, J.A.; Elvidge, C.D. Estimating population and energy consumption in Brazilian Amazonia using DMSP night-time satellite data. *Comput. Environ. Urban Syst.* **2005**, *29*, 179–195.
27. Sutton, P.C. Modeling population density with night-time satellite imagery and GIS. *Comput. Environ. Urban Syst.* **1997**, *21*, 227–244.
28. Coscieme, L.; Pulselli, F.M.; Bastianoni, S.; Elvidge, C.D.; Anderson, S.; Sutton, P.C. A thermodynamic geography: Night-Time satellite imagery as a proxy measure of emergy. *Ambio* **2013**, *42*, 1–11.
29. Ghosh, T.; Anderson S.J.; Elvidge, C.D.; Sutton, P.C. Using nighttime satellite imagery as a proxy measure of human well-being. *Sustainability* **2013**, *5*, 4988–5019.
30. Zhou, L.; Dickinson, R.E.; Tian, Y.; Fang, J.; Li, Q.; Kaufmann, R.K.; Tucker, C.J.; Myneni, R.B. Evidence for a significant urbanization effect on climate in China. *Proc. Natl. Acad. Sci. USA* **2004**, *101*, 9540–9544.
31. Kan, H.; Chen, B. Particulate air pollution in urban areas of Shanghai, China: Health-Based economic assessment. *Sci. Total Environ.* **2004**, *322*, 71–79.
32. National Bureau of Statistics of China. *China City Statistical Yearbook*; China Statistical Press: Beijing, China, 1995–2012.
33. National Bureau of Statistics of China. 2010 Sixth National Population Census Data Gazette (No. 1). 2011. Available online: http://www.stats.gov.cn/tjfx/jdfx/t20110428_40272_2253.htm (accessed on 12 March 2014).
34. Zhang, Q.; Seto, K.C. Can night-time light data identify typologies of urbanization? A global assessment of successes and failures. *Remote Sens.* **2013**, *5*, 3476–3494.
35. Elvidge, C.D.; Ziskin, D.; Baugh, K.E.; Tuttle, B.T.; Ghosh, T.; Pack, D.W.; Erwin, E.H.; Zhizhin, M. A fifteen year record of global natural gas flaring derived from satellite data. *Energies* **2009**, *2*, 595–622.